Characterization of Natural and Affected Environments

Contributions of Atmospheric deposition to Pb concentration and isotopic composition in Seawater and Particulate Matters in the Gulf of Aqaba, Red Sea

Chia-Te Chien, Tal Benaltabet, Adi Torfstein, and Adina Paytan

Environ. Sci. Technol., **Just Accepted Manuscript** • DOI: 10.1021/acs.est.9b00505 • Publication Date (Web): 15 May 2019

Contributions of Atmospheric deposition to Pb concentration and isotopic composition in Seawater and Particulate Matters in the Gulf of Aqaba, Red Sea

Chia-Te Chien[1,2*], Tal Benaltabet[3,4], Adi Torfstein[3,4] and Adina Paytan[5]

[1] Earth & Planetary Sciences Department, University of Santa Cruz, Santa Cruz, CA 95064, USA

[2] GEOMAR Helmholtz Centre for Ocean Research Kiel, Kiel 24105, Germany

[3] Institute of Earth Sciences, Hebrew University of Jerusalem, Jerusalem 91904, Israel

[4] Interuniversity Institute of Marine Sciences, Eilat 88103, Israel

[5] Institute of Marine Sciences, University of California, Santa Cruz, CA 95064, USA

*Corresponding authors – cchien@geomar.de

Abstract

Lead concentrations [Pb] and isotope ratios ($^{206}Pb/^{207}Pb$, $^{208}Pb/^{207}Pb$) have been measured in samples of total suspended particulate (TSP) aerosols, seawater, and suspended and sinking particles in the Gulf of Aqaba (GOA), Red Sea. Isotope ratios of Pb in seawater and in the soluble fraction of Pb in atmospheric TSP were similar suggesting TSP is an important source of Pb in this area. Pb concentrations in seawater measured in this study (max. 76.8 pmol kg^{-1}) were much lower than those recorded at the same location in 2003 – 2004 (up to 1000 pmol kg^{-1}). Changes in Pb isotope ratios in TSP depositing in these years indicate that leaded gasoline was responsible for the high dissolved Pb in GOA more than a decade ago and that recent regulation reduced Pb contamination. The similarity in Pb isotope ratios in suspended and sinking particles implies close interactions between these two size fractions. This study demonstrates the effect of phasing out of leaded gasoline on TSP and seawater Pb chemistry in the Northern GOA; the rate of change in dissolved Pb concentrations in the GOA is faster than that reported for the open ocean possibly due to higher particle scavenging and the relatively short residence time of deep water in the Basin.

Introduction

Atmospheric deposition is an important external source of trace metals to the ocean and can affect seawater chemistry and phytoplankton dynamics in the surface ocean.[1-5] Atmospheric deposition also provides particles to the ocean that can serve as ballast or aggregation nuclei and enhance the biological pump.[6, 7] Sinking mineral dust from atmospheric deposition can thus play an important role as a medium that transports elements from surface to the deep ocean.

Lead (Pb) is a toxic metal at high concentrations and is usually abounded in air pollution, and Pb isotope ratios can be used to identify and trace pollution sources.[8-11] Pb isotopes have also been used to shed light on Pb exchange between dissolved and particulate pools in the water column,[12, 13] which is an important factor that determines the residence time of Pb and its distributions in the ocean. Although Pb concentrations in aerosols and in seawater rarely approach toxic levels that can affect human health, incorporation of Pb in sediment and biological tissue can negatively impact marine life through bioaccumulation in the food chain.[14, 15] The Gulf of Aqaba (GOA) harbors a unique ecosystem including the north most extend of reef building coral with species that have a high tolerance to high temperature[16] and divers fisheries and recreational diving sites on which the local populations depend. However, increasing human activities have contributed pollutions and threaten the ecosystem in the GOA. A previous study in the Northern GOA has shown high variation of dissolved Pb concentrations [Pb] in near shore surface seawater, suggesting highly localized sources such as smelting operations, shipping, port activity and fossil fuel emissions.[17] This may be particularly important during the summer months when the water column in the GOA is stratified,[18] increasing the possibility of Pb accumulation in the surface and allowing Pb to reach high concentrations. More importantly, Pb was commonly used as an additive to gasoline worldwide in the mid-20th century. Although leaded gasoline was phased out in many western countries in the 1980s, it was still in use in early 2000s in many places in Asia and specifically in Jordan, close to our study site. It is important to understand how the effect of banning leaded gasoline is manifested in natural system with different circulation dynamics and ecosystems. Previous studies depicting how [Pb] decreased over time were primarily done in offshore open ocean settings[19, 20] and not in more coastal oligotrophic settings such as the GOA. We collected atmospheric total suspended particle (TSP) samples as well as water and particulate matter samples in August 2015 to assess possible sources of Pb to the GOA and dynamics of Pb in these different pools. These data were

compared to previously published measurements from 2003-2005 to assess changes in sources and shed light on associated processes. Specifically, TSP deposited on arid lands around the GOA may be transported to the adjacent water bodies over may years after initial deposition. This kind of secondary settlement in general is expected to prolong the effect of anthropogenic inputs particularly in arid coastal environments.[21, 22] While we aim to understand the overall status of current Pb distribution in the GOA and why it was so high, we can also evaluate the effects of the secondary settlement in the GOA.

In this study, we report [Pb] and Pb isotopic compositions ($^{206}Pb/^{204}Pb$, $^{206}Pb/^{207}Pb$, and $^{208}Pb/^{207}Pb$ ratios) together with some other trace metal concentrations in the GOA water column and in TSP from the surrounding area. We discuss the change in [Pb] concentrations since the early 2000s, following a ban in leaded gasoline in the region, changes in Pb sources to the GOA and the processes involved in controlling [Pb] and isotope ratios in the water column.

Materials and Methods

Sampling Sites

The GOA, a narrow northeastern extension of the Red Sea, is known for its steep shelf. At our study location, a water depth of 700 m is reached within 5 km offshore. The GOA is located within the rift valley at the plate boundary that connects seafloor spreading in the Red Sea with the Sagros-Taurus zone of continental collision.[23] It is surrounded by Egypt, Israel, Jordon and Saudi Arabia. Eilat in Israel and Aqaba in Jordon are the two major cities on the Northern GOA coast. The prevailing winds in the region generally blow along the axis of the Gulf from north to south.[24] There are no rivers flowing into the GOA and annual precipitation is very low, hence the majority of external Pb input is via dry atmospheric deposition or related to marine activities (shipping). The GOA is an oligotrophic basin with low productivity and it is characterized by stable stratification during the summer and deep convective mixing in the winter.[18, 25] The area receives relatively high aerosol deposition throughout the year and high deposition dust events occur frequently due to proximity to the Saharan and Arabian deserts.[26] Hence, it is an ideal place to study the impacts of atmospheric deposition on seawater Pb dynamics.

TSP Collection

Aerosol samples were collected with a TSP sampler attached to a five-meter-long pole located on the roof at the Interuniversity Institute for Marine Sciences (IUI) building in Eilat, Israel about 10 m from the coast. Three TSP samples were collected during the summer of 2015, the first representing atmospheric aerosols between July 21 and 28, the second between July 28 and August 6, and the third from August 6 to August 17. These samples were collected on acid-cleaned 47 mm polycarbonate membrane filters (Isopore™). Weights of the aerosol samples were obtained from the weight difference of the filter before and after sample collection. Half of each TSP sample was then used for soluble and non-soluble (residual) Pb concentration and isotope ratio analyses, respectively. TSP loads between January and August in 2015 were determined from samples collected by an identical second TSP collector located at the same site which was equipped with a Gelman® flow meter, as described elsewhere.[27]

Seawater and Particulate Matter Collection

Seawater samples were collected along a depth profile at station A (29°28'01.2"N 34°55'43.8"E; Fig. 1) on August 18 in 2015. Station A is located away from the narrow continental shelf (not affected by costal pollution processes) and is presentative of open water conditions in the GOA which enter the basin from the Red Sea via the straits of Tiran.[17, 28, 29] This is also a long terms monitoring sites in which many marine biogeochemical studies have been carried out over the years, allowing for assessment of temporal changes.[17, 28-30] Water samples were collected with Niskin bottles mounted on a rosette (SeaBird) during monthly water sampling cruises on the Inter University Institute (IUI) research vessel (http://www.iui-eilat.ac.il/Research/NMPAbout.aspx). Temperature, salinity and density were obtained with a CTD (SeaBird) attached to the rosette, additional hydrographic data collected between April and July 2015 was also obtained and are shown in Fig. S1. Samples were filtered in-line through acid washed and sample rinsed 0.2 μm cartridge filters (AcroPak™ 200 Capsules with Supor® Membrane) and collected in acid washed sample rinsed one litter LDPE bottles. The LDPE bottles were double bagged and stored in coolers for transportation to the clean lab, where seawater samples were acidified to pH of ~1.9 with double distilled concentrated nitric acid. To collect suspended particles in the water, three to five liters of unfiltered seawater from the same Niskin bottles were collected into plastic bottles rinsed thoroughly with sample water and suspended particles were collected via filtration on 0.45 μm polycarbonate filters. Sinking

particles were collected using sediment traps deployed just north of station A[31] on July 14 at water depths of 124, 226, 462 and 580 m and the traps were retrieved on August 18 (~ 1-month deployment). The sinking particulate material was split, freeze dried, weighted and preserved in plastic vials for later treatments. A surface sediment sample (2.5 cm deep, core top) from the sea floor at this site was retrieved using an MC-400 four-barrel multi-corer (Ocean Instruments, San Diego, CA) deployed from the IUI R/V Sam Rothberg. The surface sediment was processed in the same manner as the sinking particles described above. Note that the water column suspended particles were collected using Niskin bottles and hence could also include some large size particles while the particles collected in the sediment traps represent preferentially the largest size fraction of particles in the water, those that have efficient downward movement (sinking particles).

In addition, surface seawater (Fig. 1) was collected from ~0.5 m water depth at 14 sites in the northern GOA on August 11th using a peristaltic pump with acid cleaned Teflon tubing on a fiberglass speed boat. Surface water was filtered and stored in the same way as water collected from the depth profile.

Sample Pretreatments and Chemical Analyses

Details of sample pretreatments and chemical analyses can be found in supporting information. Briefly, we have applied different column chemistries for trace metal and Pb isotope analyses.[32, 33] Trace metal concentrations were analyzed by ICP-MS (Agilent 7500cx) and Pb isotopic compositions were analyzed by a multi collector inductively coupled mass spectrometer (MC-ICP-MS Neptune) at the Institute of Earth Sciences, Hebrew University of Jerusalem. Based on 36 NIST SRM-981 analyses, average and one standard deviation of $^{206}Pb/^{204}Pb$, $^{206}Pb/^{207}Pb$ and $^{208}Pb/^{207}Pb$ are 16.9298 ± 0.0056, 1.0936 ± 0.0001 and 2.3684 ± 0.0002, respectively (Table S2).

The Pb enrichment factor (EF) was also calculated using Equation 1:

$$EF = \frac{(\mathrm{Pb/Al})_{sample}}{(\mathrm{Pb/Al})_{upper\ crust}} \quad (1)$$

where $(Pb/Al)_{sample}$ is Pb to Al ratio in our TSP (soluble and non-soluble fractions), particulate matter, and seawater samples. $(Pb/Al)_{upper\ crust}$ is Pb to Al ratio in the average upper continental crust.[34] We use the average continental crust normalization and not local dust ratios for consistency with other studies.

Results

Pb in GOA TSP

TSP loads were 33.4, 38.6 and 41.4 μg m^{-3} for the three samples collected between July 21 and 28, July 28 and August 6, and from August 6 to August 17, respectively. Bulk Pb concentrations were 60, 167 and 99 ppm, respectively (calculated from the sum of soluble and non-soluble Pb fractions). The fraction of soluble Pb in these three samples was 84.2%, 85.5% and 82.9%, respectively. The EFs for Pb in the non-soluble fractions were low at 2.9, 5.3 and 2.3, respectively. TSP total EFs calculated from the soluble and non-soluble data were 18, 36 and 13 in the three samples, respectively. Pb isotope ratios of the soluble fraction in the three samples were 1.169, 1.157 and 1.161 for $^{206}Pb/^{207}Pb$ and 2.443, 2.432 and 2.435 for $^{208}Pb/^{207}Pb$, respectively. The non-soluble fraction Pb in the first TSP sample was lost during measurement, the second and third samples had ratios of 1.170 and 1.180 for $^{206}Pb/^{207}Pb$ and 2.442 and 2.452 for $^{208}Pb/^{207}Pb$, respectively (Table S1).

Pb distribution in the GOA

In August 2015, the GOA was well stratified, as can be seen in temperature, salinity and density profiles (Fig. S1). Dissolved [Pb] in the upper seawater layer (defined here as the upper 100 m based on the density profile at station A in August) ranged from 51.3 to 76.8 pmol kg^{-1} with an average of 61 pmol kg^{-1}. The concentrations in deeper water were lower than in the surface ranging from 35.9 to 58.3 pmol kg^{-1} (Fig. 2A). Dissolved Pb isotope ratios at station A ranged from 1.166 to 1.173 for $^{206}Pb/^{207}Pb$ and 2.433 to 2.442 for $^{208}Pb/^{207}Pb$. Pb isotope ratios were similar throughout the whole water column (Fig. 2B).

Upper layer suspended particulate matter [Pb] at station A ranged from 3.8 to 5.5 pmol kg^{-1} with an average of 4.8 pmol kg^{-1} (Fig. 2A). The concentrations in deeper water suspended particulate matter were higher than in the surface, ranging from 4.5 to 12.0 pmol kg^{-1}. Pb

concentrations in sinking particles were 31, 23, 28 and 23 ppm at 124, 226, 462 and 580 m, respectively. Suspended particles Pb isotope ratios in the upper layer ranged from 1.166 to 1.173 for $^{206}Pb/^{207}Pb$ and 2.433 to 2.437 for $^{208}Pb/^{207}Pb$ (Fig. 2B and table S1). Below 400 m, $^{206}Pb/^{207}Pb$ shifted from 1.174 at 400 m to 1.184 at 700 m and $^{208}Pb/^{207}Pb$ shifted from 2.440 to 2.450. In sinking particles, $^{206}Pb/^{207}Pb$ ranged from 1.172 to 1.180 and $^{208}Pb/^{207}Pb$ from 2.439 to 2.446 (Fig. 2B and table S1). Pb isotope ratios in surface sediment were 1.223 and 2.483 for $^{206}Pb/^{207}Pb$ and $^{206}Pb/^{207}Pb$, respectively.

Discussion

Pb input to the GOA from atmospheric deposition of TSP

Previous studies reported that the dominant air masses over the GOA originate from European and Mediterranean Sea sources for the majority of time (69%) and that the TSP load associated with these air masses ranges between 20 and 40 μg m^{-3}.[26] During winter and spring air masses originating from the Sahara Desert, Arabian Peninsula and from local sources become more prevalent and these air masses carry higher TSP load (> 60 μg m^{-3}).[26, 27] TSP load levels between January and August in 2015 (Fig. S2) were consistent with the previously reported range. However, higher TSP loads were found during February and March while there were only few small dust events between April and August 2015. These data suggest that while overall average annual TSP levels are similar between years the seasonal distribution of dust events can vary considerably between years.

The total TSP EFs for Pb in our samples ranged from 13 to 36, which is within the range of 2.5 to 230 (average 28) reported in a previous study for this area.[26] This EF is above the average upper crust value, indicating that anthropogenic inputs contribute to the Pb in TSP. The non-soluble fraction of Pb in TSP has an average EFs of 3.5 which is within the range of expected concentrations for mineral dust (<10). The higher EF in total TSP implies that the anthropogenic component of Pb in TSP is substantially more soluble and readily released from the bulk aerosol sample than Pb associated with the mineral dust component.

Anthropogenic sources of Pb in Israel including those originating locally and arriving from neighboring foreign countries typically ranges from 1.115 to 1.160 in $^{206}Pb/^{207}Pb$,[35] while natural Pb in the soil has $^{206}Pb/^{207}Pb$ that ranges from 1.206 to 1.219.[36] Typically, the seawater

soluble fraction of aerosol tends to have a more anthropogenic Pb isotopic signature than the non-soluble fraction.[37] This behavior can also be found in our samples where $^{206}Pb/^{207}Pb$ in the soluble fraction ranges from 1.157 to 1.167, while it ranged from 1.170 to 1.180 in the non-soluble fraction, shifting towards the natural soil Pb values of 1.206 to 1.219.

Seawater Pb concentrations in the GOA

Despite the overall high atmospheric deposition in the GOA, compared to other oceanic settings, the [Pb] we measured in the water column are not particularly high and are in fact at the very low range of values previously measured for this location.[17] The reported Pb concentrations measured in 2004-2005 ranged from 45 to 1000 pmol kg^{-1} with an average of 300 pmol kg^{-1} in the surface water at the same sampling location as those collected in our study (station A). Specifically, in our study, at station A, [Pb] ranged between 51.3 and 76.8 pmol kg^{-1} in the upper layer of the water column (0 – 100 m) and concentrations were lower ranging between 35.9 and 58.3 pmol kg^{-1} at depth (Fig. 2A). These low concentrations are comparable to those reported for open waters of the Atlantic[19] and Indian[38] ocean's surface water, and are even lower than reported [Pb] for surface water in the North Pacific.[33, 39]

To understand why [Pb] has decreased over the last decade and why the concentrations are low, it is important to (1) estimate the contribution of TSP deposition to the seawater Pb, since TSP is the major source of trace metals including Pb and (2) to shed light on internal Pb cycling within the water column after deposition. To calculate the contribution of Pb from TSP deposition we assume that the upper water column in the GOA is well mixed during winter, homogenizing [Pb] and setting the concentration to the values seen in deep water (42.9 pmol kg^{-1}); we also assume that stratification started in mid-April and was maintained until the early fall, as evident from our CTD data (Fig. S1). We further assume that atmospheric TSP adds soluble Pb immediately upon deposition into the surface water; this is supported by a previous dissolution study that showed most of TSP soluble Pb dissolved into seawater after 10 mins of seawater exposure.[40] Under these conditions the soluble Pb accumulates in the stratified layer and only particles sink into the deep water (Fig. 3). The contribution of Pb from TSP deposition

238 (Pb_d (pmol)) can then be calculated by documenting changes in surface seawater Pb
239 concentration (ΔPb_{sw} (pmol kg^{-1})) during the stratified months using the following equation:

240 $$\Delta Pb_{sw} = \frac{Pb_d}{Mass_{sw}} = \frac{Pb_a \times Pb_s \times V_d \times T}{MLD_{sw} \times D_{sw}} \quad (2)$$

241

242 Where Pb_a (pmol m^{-3}) and Pb_s (pmol $pmol^{-1}$) are Pb concentration in the air and solubility
243 of the TSP, V_d (m s^{-1}) is the deposition velocity of TSP and T (s) stands for the period of TSP
244 deposition. The product of these values, Pb_d, stands for the amount of soluble Pb from TSP
245 deposition per unit area, integrated over a certain period. MLD_{sw} (m) is the mixed layer depth
246 and D_{sw} (kg m^{-3}) is seawater density. The product, $Mass_{sw}$ (kg), is the seawater mass per unit area
247 in the mixed layer. Note that this equation calculates ΔPb_{sw} due to TSP deposition and does not
248 account for Pb removal processes in the water column such as scavenging by particles. Since we
249 collected seawater samples on the 18th of August, we assumed that the Pb increase in the surface
250 layer represents the integrated effect of deposition over the 4 months between the onset of
251 stratification and our sampling. We use the average TSP loads from mid-April to mid-August
252 (39.8 μg m^{-3}, Fig. S2), and average concentration and solubility of Pb in the samples we
253 collected for the calculation. Based on the [Pb] profile at station A that shows higher [Pb] in the
254 upper 100 m, we use this depth as the water depth affected by TSP Pb input. Using 1028 kg m^{-3}
255 as seawater density and a deposition velocity at 0.02 m s^{-1} for mineral dust,[1] we determined that
256 TSP deposition can account for a 36.1 pmol kg^{-1} increase in seawater [Pb] in the upper 100 m
257 layer from mid-April to mid-August, which is about double of the observed 18.1 pmol kg^{-1}
258 increase we recorded, based on the average [Pb] difference between the upper layer (0 – 100 m)
259 and the deep layer (below 100 m) (i.e.: observed ΔPb = [Pb in the upper layer] – [Pb in the deep
260 layer]). In addition, this is only the contributions from TSP and did not account for other local
261 inputs such as ship activity, which means the difference between observed [Pb] and total Pb flux
262 could be even larger. One possible reason for this inconsistency can be due to an over estimation
263 of the deposition rate, although similar deposition rates were observed at other locations in
264 Israel[41] and are used regularly. If we assume that the soluble Pb is associated with the
265 anthropogenic fraction which is preferentially present in the fine mode (<2 μm)[42] and use a
266 deposition velocity of 0.0036 m s^{-1},[26] in other word, assume all soluble Pb is in fine mode, we get
267 a 6.4 pmol kg^{-1} increase in [Pb]. Alternatively, the observed 18.1 pmol kg^{-1} increase in the upper

layer could be achieved at a TSP deposition velocity of 0.0102 m s^{-1}. Based on the deposition velocities for mineral dust (0.02 m s^{-1}) and for find mode (0.0036 m s^{-1}), at this velocity 60% of the Pb would be in the fine mode. Another potential explanation for the lower [Pb] that expected based on the calculation using a sinking velocity of 0.02 m s^{-1} could be high scavenging rates of Pb in the GOA. In contrast to the low concentration of Pb in seawater, suspended particles Pb concentrations were high when compared to other systems, ranging from 3.8 to 12 pmol kg^{-1}, which based on the suspended particulate matter concentration in the water column can account for 6 to 27% of the total Pb in seawater. For example, in the north Atlantic Ocean suspended Pb concentrations were typically ≤ 3 pmol kg^{-1} and constituted about 1 to 15% of total seawater Pb concentration.[12, 43] Hence, higher particle content and higher scavenging rates of Pb onto these particles can not only explain the lower than expected increase in surface Pb concentrations we observed, but it also explains the overall low Pb concentration in the GOA.

Phasing Out of Leaded Gasoline.

Although high scavenging can explain the low [Pb] recorded in 2015, it does not answer the question why [Pb] were much higher a decade before (2003 - 2005) at the very same location.[17] During 2003 to 2005, seawater at station A was collected and analyzed with similar sampling technique and analytical processes used here, and the authors reported very low contamination and validated their data using reference materials.[17] However, the reported [Pb] reached up to 1000 pmol kg^{-1} in 2003, while the highest value we observed in 2015 was only 76.8 pmol kg^{-1} (Fig. 4). Average TSP loads were 54.7 μg m^{-3} from Aug 2003 to Nov 2004[26] which is only ~26% higher than the average value of 40.6 μg m^{-3} measured between April and Aug in 2015, thus differences in Pb deposition from atmospheric TSP cannot explain the large difference in seawater [Pb] between these records.

We suggest that the change can be attributed to differences in local input of Pb from fossil fuel use. Surface water [Pb] in the north-western corner of the GOA within Israel's waters in August of 2015 (Fig. 1B) ranged from 37.4 to 93.4 pmol kg^{-1}, with the highest values observed at the northern coastal sites. This is where the city of Eilat is located with a larger density of population and hotels compared to other coastal sites along the GOA and the main harbors of Eilat, thus this area is more likely to be affected from higher local anthropogenic sources of Pb. The higher [Pb] are associated with higher $^{206}Pb/^{207}Pb$ and $^{206}Pb/^{204}Pb$ ratios,

298 reaching 1.189 and 18.58, respectively, while the sites further south and offshore have ratios
299 around 1.180 and 18.4. Although higher [Pb] typically indicate higher anthropogenic inputs the
300 higher $^{206}Pb/^{207}Pb$ ratio of these samples suggest a natural signature. Since the northern coastal
301 area is much shallower (<50 m), groundwater inputs typically are higher within these sites and
302 can contribute more Pb.[44] While some spatial variability is seen, surface concentrations of Al,
303 Mn, Co, Zn and Cd were also higher in the north part of the GOA (Fig. S3). A local input from
304 contaminated groundwater or other urban activity related point sources can also explain why the
305 local higher Pb "hot-spots" are confined to the most north part of the GOA and do not affect sites
306 that are away from the coast including offshore locations such as station A (Fig. 1B). Figure S4
307 shows concentration profiles of Al, Mn, Co, Zn and Cd at station A and they are very similar to
308 those measured more than a decade ago.[17] This offset in temporal trends between Pb and the
309 other metals suggests that the observed decline in [Pb] particularly offshore cannot be attributed
310 to changes in local contaminant inputs of Pb, because such contaminations are usually also
311 associate with high levels of other metals such as Zn and Cd.[45, 46] Hence a reduction in a source
312 that preferentially affects Pb is a more likely explanation.
313 We use the Pb isotope data to identify possible sources of [Pb] that could explain the
314 reduction in Pb concentration. Figure 5 is a triple Pb isotope plot ($^{208}Pb/^{207}Pb$ vs. $^{206}Pb/^{207}Pb$) and
315 it includes the published ratios associated with different sources of Pb including mineral brine,
316 soil, aerosol (TSP), leaded gasoline as well as seawater dissolved and particulate Pb from this
317 study (Fig. 5B). The Pb isotope ratios associated with TSP collected in 2015 (avg. $^{206}Pb/^{207}Pb$ =
318 1.167, $^{208}Pb/^{207}Pb$ = 2.437) are very different from those collected between 1994 to 1998 in Israel
319 and nearby countries (avg. $^{206}Pb/^{207}Pb$ = 1.138, $^{208}Pb/^{207}Pb$ = 2.412).[35, 47] Samples collected in
320 the 1990s were largely impacted by leaded gasoline (avg. $^{206}Pb/^{207}Pb$ = 1.109, $^{208}Pb/^{207}Pb$ =
321 2.384).[35] Samples collected during 2001 to 2003[48] had a high variation in Pb isotope ratios,
322 $^{206}Pb/^{207}Pb$ ranged from 1.131 to 1.188 and $^{208}Pb/^{207}Pb$ from 2.402 to 2.472 for the acid leach
323 fraction, and in the residue $^{206}Pb/^{207}Pb$ ranged from 1.126 to 1.193 and $^{208}Pb/^{207}Pb$ from 2.400 to
324 2.477 (Fig. 5). This indicates that both the acid leach and residual fractions were contaminated
325 by leaded gasoline, but the overall ratios were already shifted slightly away from the leaded
326 gasoline value itself, this reflects the onset of banning leaded gasoline in 1994 in Israel and the
327 following decrease of Pb contaminations. As of 2005 leaded gasoline was still in use in Egypt
328 and Jordan and although in Israel phasing out started in 1994, it was not fully phased out until

2004,[49] we argue that the high soluble Pb found in the GOA during 2003 to 2005 was due to high Pb input from leaded gasoline that was transported via atmospheric TSP to the region. At present, leaded gasoline is already phased out in all countries surrounding the GOA and in most of the countries in west Asia and Africa,[50] hence the impact of gasoline use on Pb in TSP, and hence in seawater in the GOA, is expected to be significantly lower than prior to this phase-out. The low [Pb] in the GOA also suggests that although transport of Pb contaminated particles that were previously deposited on land cannot be ruled out and is expected in arid areas, this process contributes at present much less Pb to seawater in the GOA than the combined inputs from leaded gasoline more than a decade ago.

Interestingly, we found that Pb isotope ratios in the Arabian Sea seawater collected between 2009 and 2010 (avg. $^{206}Pb/^{207}Pb = 1.145$, $^{208}Pb/^{207}Pb = 2.426$, 0 – 200 m at stations 5, 6, 7 and 8 in Lee et al. 2015), falls closer to those of leaded gasoline than what we recorded in the northern GOA in 2015 (Fig. 5). It is possible that because the samples from the Indian Ocean were collected more than five years earlier than our samples, they still contained a higher signature from leaded gasoline. Alternatively, it is also possible that higher removal rates of Pb in the GOA eliminated the leaded gasoline signature faster than in the Indian Ocean. The deep mixing that occurs in the GOA and the relatively short residence time of water in the GOA also contribute to signal dilution and fast removal, respectively, in the GOA.[51] This also explains the large temporal variability in the GOA data set from 2003 -2005 which includes some periods with low [Pb] which could be explained by different contributions form TSP and particle transport from land and annual differences in both TSP deposition and mixing depth (Fig. 4).

Change over time of seawater Pb isotope ratios has been studied using Pb in coral skeletons.[52-57] In the north Atlantic, a dramatic shift in Pb isotope ratios has been recorded post leaded gasoline banning in North America.[53-55] Seawater Pb concentrations also decreased from about 200 pmol kg^{-1} in mid 1970s to 40 pmol kg^{-1} in the end of the 20^{th}.[54] This change is slower than that observed in the GOA, likely because Pb removal processes other than particle scavenging (deep water column missing and relatively fast water exchange in the GOA) are not operating in the open ocean.

Particles dynamic in the GOA

Figure 5 demonstrates that Pb isotopes in seawater and in particulate matters in the GOA

are likely attributed to a mixture of Pb originating from TSP and Pb originating from natural local sources such as soil. Figure 2 shows that in the upper water layer, Pb isotopes ratios in suspended particles and those of Pb dissolved in seawater are similar to each other although the isotope ratios of the soluble and non-soluble fractions of TSP are distinct. The similarity between the dissolved and suspended Pb isotopes suggest that there is fast exchange between these two fractions (through adsorption and desorption processes onto/off particle surfaces) and that Pb has reached equilibrium.[58] Since the water during our sampling in August 2015 has been stratified for a few months the similarity sets an upper limit of the exchange/equilibrium rate. Below 400 m, the Pb isotope ratios in suspended particles deviated from those in seawater. In the bottom layer between 400 m and 700 m, $^{206}Pb/^{207}Pb$ in suspended particles shift from 1.174 to 1.184 and $^{208}Pb/^{207}Pb$ shifted from 2.440 to 2.450. (Fig. 2B). One explanation could be that due to resuspension of sediments at the bottom or lateral particle transport from the steep slope of the GOA introduce new particles to the water column. Sediment resuspension contributed 20% of the suspended particles at 700 m ($^{206}Pb/^{207}Pb = 1.184$) based on a simple mixture of $^{206}Pb/^{207}Pb$ ratios between the particles at 400 m ($^{206}Pb/^{207}Pb = 1.174$) and those in the surface sediments ($^{206}Pb/^{207}Pb = 1.223$). However, the suspended particle concentrations at these depths were not higher than those at other depths (Fig. 2A) and did not indicate new particle sources, however, a shorter residence time of the particles due to a higher removal rate could reconcile the divergence of concentrations and isotopes profiles (Fig. 2). The deviation in isotope signature between the dissolved and suspended particle Pb isotope ratios implies a short residence time of these resuspended particles (less than the stratification time) since they did reach equilibrium with seawater dissolved Pb in the upper layer. Alternatively, it may be that the resuspended particles have different surface characteristics with adsorption/desorption rates that differ from suspended particles in the shallower section.

Pb isotope ratios in sinking particles are similar to those in suspended particles, common sources and constant aggregation and disaggregation resulting in close interaction between different particle size groups can explain these observations. It is also possible that the Pb isotopes of both particles sources is similar, whether the source is from sediment resuspension or lateral transportation.

In this study based on Pb mass balance calculations, EFs, and the similarity in Pb isotopes between the soluble fraction of Pb in TSP and dissolved [Pb] in seawater we suggest that atmospheric deposition of TSP is an important source of dissolved Pb to the GOA. Evidence of changes in [Pb] in surface waters between 2005 and 2015, coupled with Pb isotope signatures of potential sources of Pb in the region suggests that leaded gasoline transported via TSP was a major source Pb in the GOA. This is the reason that while TSP loads in 2015 are similar to those in 2003 to 2005, [Pb] were much lower and less variable in 2015 after leaded gasoline use in the region was phased-out. Further, Pb isotopes in dissolved and suspended particles indicate that scavenging rate of Pb by particles and adsorption/desorption processes, particularly in the upper water column, are high in the GOA.

Acknowledgments

We thank the IUI marine crew and technical staff for their assistance and hospitality. We further wish to thank Ofir Tirosh at HUJI for his dedication and help with sample analyses. This work is a part of International Experience for Students in Coastal Zone Research (IRES) project # OIA-IRES 1358134 to AP funded by the NSF. Additional funding was provided to AT by Israel Science Foundation grant #927/15 and the Ring Foundation.

Supporting Information

Sample Pretreatments and Chemical Analyses, Pb isotopes data for this study, evaluation of Pb isotopes analyses and column chemistry, basic hydrology data at the study site, records of atmospheric TSP loads at the study area, trace metal concentrations in the GOA in 2015, Comparison of trace metal profiles at our study site in different years.

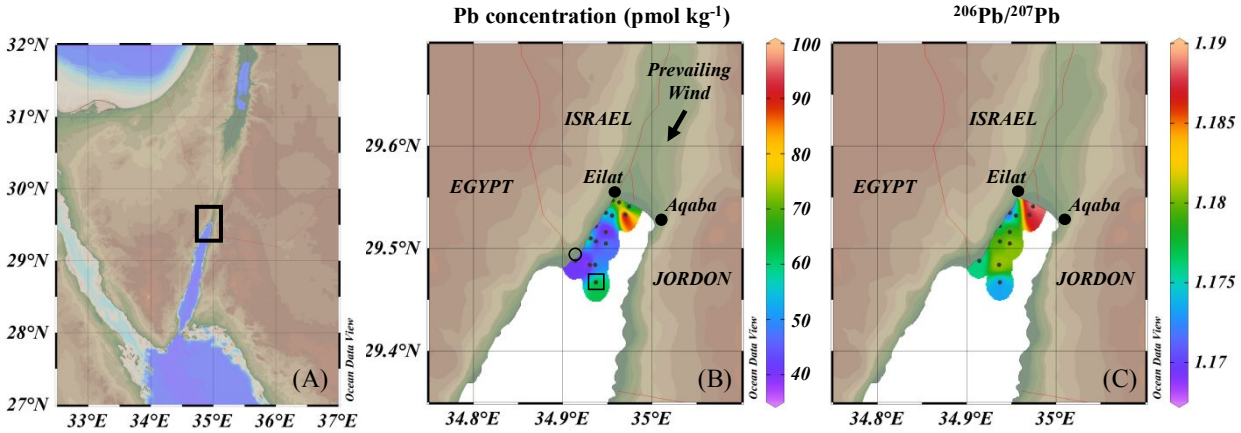

Figure 1. Location of samples collected in the northern GOA (A) and Pb concentration (B) and $^{206}Pb/^{207}Pb$ (C) in surface water at the study area. Black dots mark the surface sampling sites, open square station A depth profile, and open circle the TSP sampling site. Figure 1 was prepared with Ocean Data View.[59]

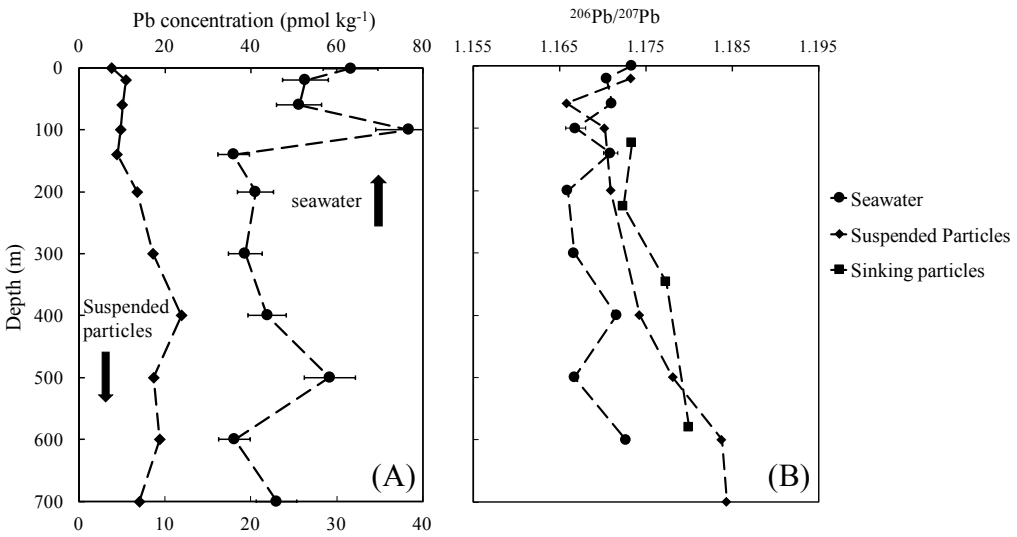

Figure 2. Pb concentrations (A) and isotope ratios (B) in seawater, suspended and sinking particles collected in August 2015. Note that the arrows in the concentration figure point seawater and suspended particles to different scales.

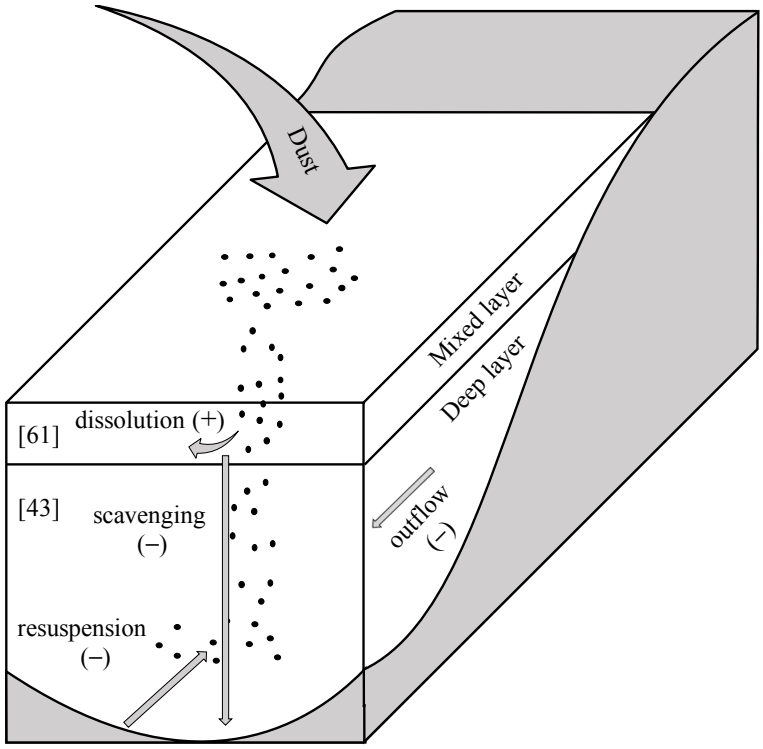

Figure 3. A schematic diagram showing how TSP contributes dissolved Pb to the upper layer of the water column in the GOA and the particle dynamics in the water column. Numbers in brackets are [Pb] concentrations in the upper mixed layer and deep layer.

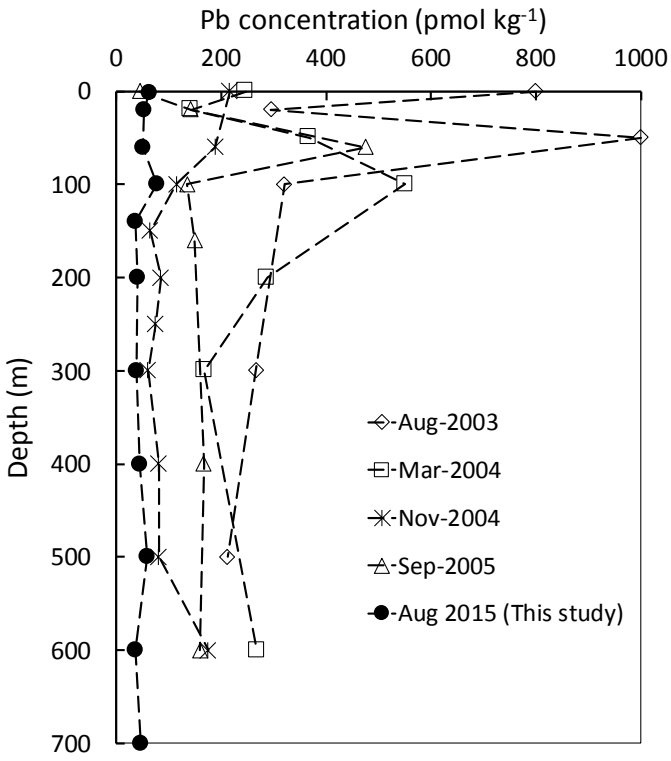

423

424 Figure 4. Pb profiles at station A in GOA collected in 2015 (solid circle, this study) and during

425 2003 to 2005 during different seasons.[17]

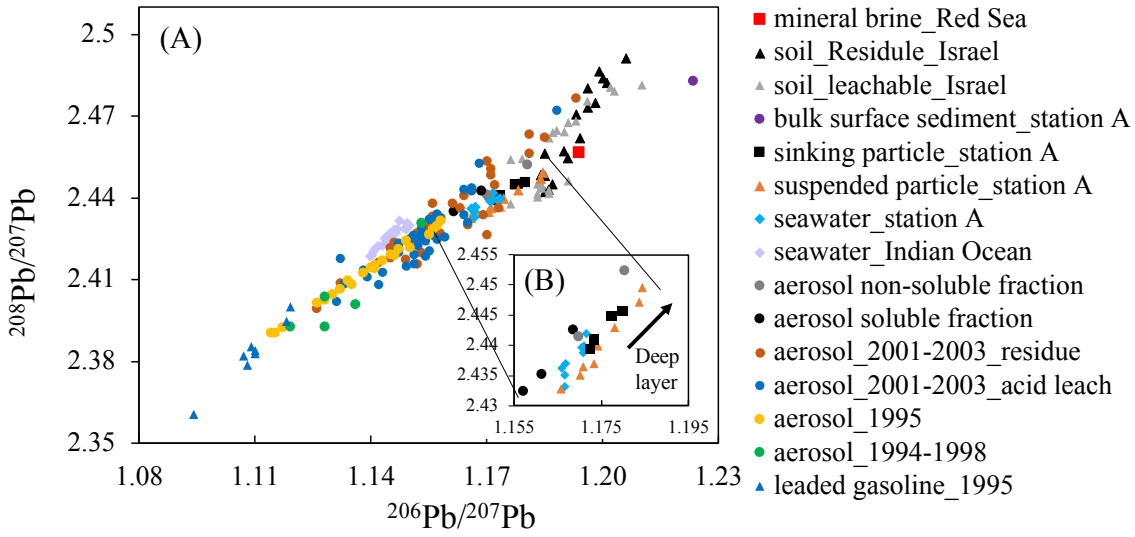

Figure 5. A triple Pb isotope plot for dissolved Pb in in seawater, suspended and sinking particles, surface sediments (2.5 cm deep), soluble and non-soluble fraction of TSP in this study, mineral brine in the Red Sea region,[60] soil acid leach and residue fractions,[35] Indian Ocean seawater (0 – 200 m at stations 5, 6, 7 and 8),[61] aerosol collected in Israel and nearby countries, [47] aerosols and leaded gasoline collected in Israel in 1995 and aerosol in 2001-2003.[35, 48]

Reference

1. Duce, R. A.; Liss, P. S.; Merrill, J. T.; Atlas, E. L.; Buat-Menard, P.; Hicks, B. B.; Miller, J. M.; Prospero, J. M.; Arimoto, R.; Church, T. M.; Ellis, W.; Galloway, J. N.; Hansen, L.; Jickells, T. D.; Knap, A. H.; Reinhardt, K. H.; Schneider, B.; Soudine, A.; Tokos, J. J.; Tsunogai, S.; Wollast, R.; Zhou, M., The atomspheric input of trace species to the world ocean. *Glob. Biogeochem. Cycles* **1991,** *5*, (3), 193-260.
2. Guo, C.; Yu, J.; Ho, T. Y.; Wang, L.; Song, S.; Kong, L.; Liu, H., Dynamics of phytoplankton community structure in the South China Sea in response to the East Asian aerosol input. *Biogeosciences* **2012,** *9*, (4), 1519-1536.
3. Jordi, A.; Basterretxea, G.; Tovar-Sánchez, A.; Alastuey, A.; Querol, X., Copper aerosols inhibit phytoplankton growth in the Mediterranean Sea. *Proc. Natl. Acad. Sci. U.S.A.* **2012**.
4. Mackey, K. R.; Buck, K. N.; Casey, J. R.; Cid, A.; Lomas, M. W.; Sohrin, Y.; Paytan, A., Phytoplankton responses to atmospheric metal deposition in the coastal and open-ocean Sargasso Sea. *Front. Microbiol.* **2012,** *3*, 359.
5. Chien, C.-T.; Mackey, K. R. M.; Dutkiewicz, S.; Mahowald, N. M.; Prospero, J. M.; Paytan, A., Effects of African dust deposition on phytoplankton in the western tropical Atlantic Ocean off Barbados. *Glob. Biogeochem. Cycles* **2016,** *30*, (5), 716-734.
6. Pabortsava, K.; Lampitt, R. S.; Benson, J.; Crowe, C.; McLachlan, R.; Le Moigne, F. A. C.; Mark Moore, C.; Pebody, C.; Provost, P.; Rees, A. P.; Tilstone, G. H.; Woodward, E. M. S., Carbon sequestration in the deep Atlantic enhanced by Saharan dust. *Nature Geosci.* **2017,** *10*, (3), 189-194.
7. Baker, A. R.; Landing, W. M.; Bucciarelli, E.; Cheize, M.; Fietz, S.; Hayes, C. T.; Kadko, D.; Morton, P. L.; Rogan, N.; Sarthou, G.; Shelley, R. U.; Shi, Z.; Shiller, A.; van Hulten, M. M. P., Trace element and isotope deposition across the air–sea interface: progress and research needs. *Phil. Trans. R. Soc. A* **2016,** *374*, (2081), 20160190.
8. Chow, T. J.; Johnstone, M. S., Lead Isotopes in Gasoline and Aerosols of Los Angeles Basin, California. *Science* **1965,** *147*, (3657), 502-503.
9. Flegal, A. R.; Schaule, B. K.; Patterson, C. C., Stable isotopic ratios of lead in surface waters of the Central Pacific. *Mar. Chem.* **1984,** *14*, (3), 281-287.
10. Harlavan, Y.; Almogi-Labin, A.; Herut, B., Tracing Natural and Anthropogenic Pb in Sediments along the Mediterranean Coast of Israel Using Pb Isotopes. *Environ. Sci. Technol.* **2010,** *44*, (17), 6576-6582.
11. Maring, H.; Settle, D. M.; Buat-Ménard, P.; Dulac, F.; Patterson, C. C., Stable lead isotope tracers of air mass trajectories in the Mediterranean region. *Nature* **1987,** *330*, (6144), 154-156.
12. Sherrell, R. M.; Boyle, E. A.; Hamelin, B., Isotopic equilibration between dissolved and suspended particulate lead in the Atlantic Ocean: Evidence from 210Pb and stable Pb isotopes. *J. Geophys. Res.: Oceans.* **1992,** *97*, (C7), 11257-11268.
13. Wu, J.; Rember, R.; Jin, M.; Boyle, E. A.; Flegal, A. R., Isotopic evidence for the source of lead in the North Pacific abyssal water. *Geochim. Cosmochim. Acta* **2010,** *74*, (16), 4629-4638.
14. Bryan, G. W.; Langston, W. J., Bioavailability, accumulation and effects of heavy metals in sediments with special reference to United Kingdom estuaries: a review. *Environ. Pollut.* **1992,** *76*, (2), 89-131.
15. Dang, D. H.; Schäfer, J.; Brach-Papa, C.; Lenoble, V.; Durrieu, G.; Dutruch, L.; Chiffoleau, J.-F.; Gonzalez, J.-L.; Blanc, G.; Mullot, J.-U.; Mounier, S.; Garnier, C., Evidencing the Impact of Coastal Contaminated Sediments on Mussels Through Pb Stable Isotopes Composition. *Environ. Sci. Technol.* **2015,** *49*, (19), 11438-11448.
16. Krueger, T.; Horwitz, N.; Bodin, J.; Giovani, M.-E.; Escrig, S.; Meibom, A.; Fine, M., Common reef-building coral in the Northern Red Sea resistant to elevated temperature and acidification. *Royal Society Open Science* **2017,** *4*, (5), 170038.

17. Chase, Z.; Paytan, A.; Beck, A.; Biller, D.; Bruland, K.; Measures, C.; Sañudo-Wilhelmy, S., Evaluating the impact of atmospheric deposition on dissolved trace-metals in the Gulf of Aqaba, Red Sea. *Mar. Chem.* **2011,** *126*, (1–4), 256-268.
18. Biton, E.; Gildor, H., Stepwise seasonal restratification and the evolution of salinity minimum in the Gulf of Aqaba (Gulf of Eilat). *J. Geophys. Res.: Oceans.* **2011,** *116*, (C8), n/a-n/a.
19. Bridgestock, L.; van de Flierdt, T.; Rehkämper, M.; Paul, M.; Middag, R.; Milne, A.; Lohan, M. C.; Baker, A. R.; Chance, R.; Khondoker, R.; Strekopytov, S.; Humphreys-Williams, E.; Achterberg, E. P.; Rijkenberg, M. J. A.; Gerringa, L. J. A.; de Baar, H. J. W., Return of naturally sourced Pb to Atlantic surface waters. *Nature Commun.* **2016,** *7*, 12921.
20. Lee, J. M.; Boyle, E. A.; Echegoyen-Sanz, Y.; Fitzsimmons, J. N.; Zhang, R.; Kayser, R. A., Analysis of trace metals (Cu, Cd, Pb, and Fe) in seawater using single batch nitrilotriacetate resin extraction and isotope dilution inductively coupled plasma mass spectrometry. *Anal. Chim. Acta* **2011,** *686*, (1-2), 93-101.
21. Harris, A. R.; Davidson, C. I., The Role of Resuspended Soil in Lead Flows in the California South Coast Air Basin. *Environ. Sci. Technol.* **2005,** *39*, (19), 7410-7415.
22. Laidlaw, M. A. S.; Zahran, S.; Mielke, H. W.; Taylor, M. P.; Filippelli, G. M., Re-suspension of lead contaminated urban soil as a dominant source of atmospheric lead in Birmingham, Chicago, Detroit and Pittsburgh, USA. *Atmos. Environ.* **2012,** *49*, 302-310.
23. Ben-Avraham, Z., Structural framework of the Gulf of Elat (AQABA), Northern Red Sea. *Journal of Geophysical Research: Solid Earth* **1985,** *90*, (B1), 703-726.
24. Genin, A.; Paldor, N., Changes in the circulation and current spectrum near the tip of the narrow, seasonally mixed Gulf of Elat. *Isr. J. Earth Sci.* **1998,** *47*, 87-92.
25. Biton, E.; Gildor, H., The general circulation of the Gulf of Aqaba (Gulf of Eilat) revisited: The interplay between the exchange flow through the Straits of Tiran and surface fluxes. *J. Geophys. Res.: Oceans.* **2011,** *116*, (C8), n/a-n/a.
26. Chen, Y.; Paytan, A.; Chase, Z.; Measures, C.; Beck, A. J.; Sañudo-Wilhelmy, S. A.; Post, A. F., Sources and fluxes of atmospheric trace elements to the Gulf of Aqaba, Red Sea. *J. Geophys. Res. Atmos.* **2008,** *113*, (D5), D05306.
27. Torfstein, A.; Teutsch, N.; Tirosh, O.; Shaked, Y.; Rivlin, T.; Zipori, A.; Stein, M.; Lazar, B.; Erel, Y., Chemical characterization of atmospheric dust from a weekly time series in the north Red Sea between 2006 and 2010. *Geochim. Cosmochim. Acta* **2017,** *211*, (Supplement C), 373-393.
28. Shaked, Y., Iron redox dynamics in the surface waters of the Gulf of Aqaba, Red Sea. *Geochim. Cosmochim. Acta* **2008,** *72*, (6), 1540-1554.
29. Chase, Z.; Paytan, A.; Johnson, K. S.; Street, J.; Chen, Y., Input and cycling of iron in the Gulf of Aqaba, Red Sea. *Glob. Biogeochem. Cycles* **2006,** *20*, (3), GB3017.
30. Lindell, D.; Post, A. F., Ultraphytoplankton succession is triggered by deep winter mixing in the Gulf of Aqaba (Eilat), Red Sea. *Limnol. Oceanogr.* **1995,** *40*, (6), 1130-1141.
31. Chernihovsky, N.; Torfstein, A.; Almogi-Labin, A., Seasonal flux patterns of planktonic foraminifera in a deep, oligotrophic, marginal sea: Sediment trap time series from the Gulf of Aqaba, northern Red Sea. *Deep Sea Res., Part I* **2018,** *140*, 78-94.
32. Sohrin, Y.; Urushihara, S.; Nakatsuka, S.; Kono, T.; Higo, E.; Minami, T.; Norisuye, K.; Umetani, S., Multielemental determination of GEOTRACES key trace metals in seawater by ICPMS after preconcentration using an ethylenediaminetriacetic acid chelating resin. *Anal. Chem.* **2008,** *80*, (16), 6267-6273.
33. Chien, C.-T.; Ho, T.-Y.; Sanborn, M. E.; Yin, Q.-Z.; Paytan, A., Lead concentrations and isotopic compositions in the Western Philippine Sea. *Mar. Chem.* **2017,** *189*, 10-16.
34. Taylor, S. R.; McLennan, S. M., The continental crust: its composition and evolution. **1985**.

35. Erel, Y.; Veron, A.; Halicz, L., Tracing the transport of anthropogenic lead in the atmosphere and in soils using isotopic ratios. *Geochim. Cosmochim. Acta* **1997,** *61*, (21), 4495-4505.
36. Teutsch, N.; Erel, Y.; Halicz, L.; Banin, A., Distribution of natural and anthropogenic lead in Mediterranean soils. *Geochim. Cosmochim. Acta* **2001,** *65*, (17), 2853-2864.
37. Hsu, S.-C.; Lin, F.-J.; Jeng, W.-L., Seawater solubility of natural and anthropogenic metals within ambient aerosols collected from Taiwan coastal sites. *Atmos. Environ.* **2005,** *39*, (22), 3989-4001.
38. Echegoyen, Y.; Boyle, E. A.; Lee, J. M.; Gamo, T.; Obata, H.; Norisuye, K., Recent distribution of lead in the Indian Ocean reflects the impact of regional emissions. *Proc Natl Acad Sci U S A* **2014,** *111*, (43), 15328-31.
39. Zurbrick, C. M.; Gallon, C.; Flegal, A. R., Historic and Industrial Lead within the Northwest Pacific Ocean Evidenced by Lead Isotopes in Seawater. *Environ. Sci. Technol.* **2017,** *51*, (3), 1203-1212.
40. Mackey, K. R. M.; Chein, C.-T.; Post, A. F.; Saito, M. A.; Paytan, A., Rapid and gradual modes of aerosol trace metal dissolution in seawater. *Front. Microbiol.* **2015,** *5*.
41. Ganor, E.; Foner, H. A., Mineral dust concentrations, deposition fluxes and deposition velocities in dust episodes over Israel. *J. Geophys. Res. Atmos.* **2001,** *106*, (D16), 18431-18437.
42. Chance, R.; Jickells, T. D.; Baker, A. R., Atmospheric trace metal concentrations, solubility and deposition fluxes in remote marine air over the south-east Atlantic. *Mar. Chem.* **2015,** *177, Part 1*, 45-56.
43. Noble, A. E.; Echegoyen-Sanz, Y.; Boyle, E. A.; Ohnemus, D. C.; Lam, P. J.; Kayser, R.; Reuer, M.; Wu, J.; Smethie, W., Dynamic variability of dissolved Pb and Pb isotope composition from the U.S. North Atlantic GEOTRACES transect. *Deep Sea Res., Part II* **2015,** *116*, (Complete), 208-225.
44. Shellenbarger, G. G.; Monismith, S. G.; Genin, A.; Paytan, A., The importance of submarine groundwater discharge to the near shore nutrient supply in the Gulf of Aqaba (Israel). *Limnol. Oceanogr.* **2006,** *51*, (4), 1876-1886.
45. Chen, T.-B.; Zheng, Y.-M.; Lei, M.; Huang, Z.-C.; Wu, H.-T.; Chen, H.; Fan, K.-K.; Yu, K.; Wu, X.; Tian, Q.-Z., Assessment of heavy metal pollution in surface soils of urban parks in Beijing, China. *Chemosphere* **2005,** *60*, (4), 542-551.
46. Bilos, C.; Colombo, J. C.; Skorupka, C. N.; Rodriguez Presa, M. J., Sources, distribution and variability of airborne trace metals in La Plata City area, Argentina. *Environ. Pollut.* **2001,** *111*, (1), 149-158.
47. Bollhöfer, A.; Rosman, K. J. R., Isotopic source signatures for atmospheric lead: the Northern Hemisphere. *Geochim. Cosmochim. Acta* **2001,** *65*, (11), 1727-1740.
48. Erel, Y.; Dayan, U.; Rabi, R.; Rudich, Y.; Stein, M., Trans Boundary Transport of Pollutants by Atmospheric Mineral Dust. *Environ. Sci. Technol.* **2006,** *40*, (9), 2996-3005.
49. Israel National Report for CSD-14/15 Thematic Areas. http://www.sviva.gov.il/InfoServices/ReservoirInfo/DocLib2/Publications/P0401-P0500/P0401.pdf
50. United Nations Environment Programme. Middle East West Asia Lead Status Map **2017**, https://www.unenvironment.org/resources/report/middle-east-west-asia-lead-status-map
51. Zhai, P.; Bower, A. S.; Smethie Jr., W. M.; Pratt, L. J., Formation and spreading of Red Sea Outflow Water in the Red Sea. *J. Geophys. Res.: Oceans.* **2015,** *120*, (9), 6542-6563.
52. Shen, G. T.; Boyle, E. A., Lead in corals: reconstruction of historical industrial fluxes to the surface ocean. *Earth Planet. Sci. Lett.* **1987,** *82*, (3), 289-304.
53. Reuer, M. K.; Boyle, E. A.; Grant, B. C., Lead isotope analysis of marine carbonates and seawater by multiple collector ICP-MS. *Chemical Geology* **2003,** *200*, (1), 137-153.
54. Kelly, A. E.; Reuer, M. K.; Goodkin, N. F.; Boyle, E. A., Lead concentrations and isotopes in corals and water near Bermuda, 1780–2000. *Earth Planet. Sci. Lett.* **2009,** *283*, (1), 93-100.
55. Boyle, E. A.; Lee, J.-M.; Echegoyen, Y.; Noble, A.; Moos, S.; Carrasco, G.; Zhao, N.; Kayser, R.; Zhang, J.; Gamo, T., Anthropogenic lead emissions in the ocean – the evolving global experiment. *Oceanography* **2014**.

574 56. Inoue, M.; Tanimizu, M., Anthropogenic lead inputs to the western Pacific during the 20th
575 century. *Sci. Total Environ.* **2008,** *406*, (1), 123-130.
576 57. Lee, J.-M.; Boyle, E. A.; Suci Nurhati, I.; Pfeiffer, M.; Meltzner, A. J.; Suwargadi, B., Coral-based
577 history of lead and lead isotopes of the surface Indian Ocean since the mid-20th century. *Earth Planet.*
578 *Sci. Lett.* **2014,** *398*, 37-47.
579 58. Chen, M.; Boyle, E. A.; Lee, J.-M.; Nurhati, I.; Zurbrick, C.; Switzer, A. D.; Carrasco, G., Lead
580 isotope exchange between dissolved and fluvial particulate matter: a laboratory study from the Johor
581 River estuary. *Philosophical Transactions of the Royal Society A: Mathematical,*
582 *Physical and Engineering Sciences* **2016,** *374*, (2081).
583 59. Schlitzer, R. , Ocean Data View, https://odv.awi.de, **2018**.
584 60. Delevaux, M. H.; Doe, B. R.; Brown, G. F., Preliminary lead isotope investigations of brine from
585 the Red Sea, Galena from the Kingdom of Saudi Arabia, and galena from United Arab Republic (Egypt).
586 *Earth Planet. Sci. Lett.* **1967,** *3*, 139-144.
587 61. Lee, J.-M.; Boyle, E. A.; Gamo, T.; Obata, H.; Norisuye, K.; Echegoyen, Y., Impact of
588 anthropogenic Pb and ocean circulation on the recent distribution of Pb isotopes in the Indian Ocean.
589 *Geochim. Cosmochim. Acta* **2015,** *170*, 126-144.
590